IOP Conf. Series: Materials Science and Engineering **779** (2020) 012047 doi:10.1088/1757-899X/779/1/012047

Hydrodynamic modeling of cavitation in a multistage centrifugal pump during its operation in the constant feed mode with a change in the rotor speed of the pump

M Kasatkin[1] and A Petrov[1,2]

[1]Bauman Moscow State Technical University

[2]E-mail: alex_i_petrov@mail.ru

Abstract: Hydrodynamic modeling of cavitation for a multi-section high-speed centrifugal pump operating at a constant supply is carried out. The cavitation characteristics of the pump for various pump operating modes are determined taking into account changes in the rotor speed. The operation parameters of the mobile pumping system for these modes are calculated. It has been established that improving the cavitation qualities of a pump by reducing the speed of the pump rotor with a constant flow rate is not a productive method.

Introduction

In modern mobile deployable pumping systems, in particular, in oil, fuel or water transportation systems, retaining installations are used to provide the backwater necessary for the cavitation-free operation of the main pumps. Such installations include pumps with a small allowable cavitation margin, as they are required to collect the pumped liquid from various containers in which the liquid level may be below the level of the suction pipe of the pump. The use of a retaining installation is a standard solution for the operation of mobile pumping systems for various liquids, but in this case it is required to operate 2 types of equipment: a linear pumping station and a retaining installation [1]–[4].

In this situation, it becomes urgent to reduce the range of equipment used: to make possible to operate a linear station as a retaining station. It is considered the option of reducing the pump rotor speed of a linear pumping station with a diesel engine and a multistage centrifugal pump at the same value of the liquid flow rate in the system pipeline (by regulating the operation of subsequent stations) to reduce the cavitation stock of the pump and, therefore, the operation of such a station as a booster.

The difficulty in solving the problem lies in the fact that when the speed changes while the pump supply remains constant (due to the operation of other series-connected stations), its operating mode leaves the zone of optimal operating modes. Consequently, the cavitation characteristics of the pump, increasing due to a decrease in the rotor speed, are simultaneously deteriorating due to changes in the conditions of entry into the impeller in off-design modes. Hydrodynamic modeling of a two-phase flow in the first stage of the pump should answer the question of how these two factors together affect the suction capacity of the pump.

Method

Theoretical part.

Hydrodynamic modeling is based on the following equations [5]–[9]:

- Fluid continuity equation:

$$\frac{\partial \overline{u_x}}{\partial x}+\frac{\partial \overline{u_y}}{\partial y}+\frac{\partial \overline{u_z}}{\partial z}=0,$$

Where $\overline{u_i}$ —time-averaged projections of fluid velocities on the corresponding axes.

- equation of change in momentum averaged over time:

$$\rho\left[\frac{\partial \overline{u_i}}{\partial t}+\overline{u_j}\frac{\partial \overline{u_i}}{\partial x_j}\right]=-\frac{\partial \overline{p}}{\partial x_i}+\frac{\partial}{\partial x_i}\left[T_{ij}^{(v)}-\rho u_i u_j\right],$$

Where $\overline{w_i}$ — average relative speed:

$\vec{w}=\vec{V}-\vec{u}$ — Ratio of relative, absolute and portable speed;

$\overline{p}$ — Averaged pressure;

$\tilde{T}_{ij}^{(v)}=2\mu\tilde{s}_{ij}$ — Viscous stress tensor for incompressible fluid;

$\tilde{s}_{ij}=\frac{1}{2}\left[\frac{\partial \overline{w_i}}{\partial x_j}+\frac{\partial \overline{w_j}}{\partial x_i}\right]$—deformation rate tensor;

$\rho w_i w_j$ — Reynolds stresses.

Due to the presence of Reynolds stresses, the system of equations cannot be closed. In this case, the k-ω SST turbulence model is used to close the system. A feature of this model is the combination of the advantages of both k-ω and k-ε models: the k-ε model is used in the flow core, and the k-ω model in the near-wall region.

Two equations of transport of turbulence parameters are the basis of this model:

- equation of kinetic energy transfer of turbulence:

$$\frac{\partial k}{\partial t}+\overline{u_j}\frac{\partial k}{\partial x_j}=P_k-\beta^* k\omega+\frac{\partial}{\partial x_i}\left[\left(\nu+\sigma_k\nu_T\right)\frac{\partial k}{\partial x_j}\right],$$

Where $k=\frac{\left(u_x^{'2}\right)+\left(u_y^{'2}\right)+\left(u_z^{'2}\right)}{2}$—kinetic energy of turbulence;

$u_i^{'}$—Velocity fluctuations;

P_k — Factor of turbulence energy generation;

ω — Relative turbulence dissipation rate;

ν_T — Turbulent viscosity.

- Equation of transfer of relative velocity of turbulence energy dissipation:

$$\frac{\partial \omega}{\partial t}+\overline{u_j}\frac{\partial \omega}{\partial x_j}=\alpha S^2-\beta\omega^2+\frac{\partial}{\partial x_i}\left[\left(\nu+\sigma_\omega\nu_T\right)\frac{\partial \omega}{\partial x_j}\right]+2\left(1-F_j\right)\sigma_{\omega 2}\frac{1}{\omega}\frac{\partial k}{\partial x_j}\frac{\partial \omega}{\partial x_j},$$

The Boussines q hypothesis allows us to calculate Reynolds stresses in the equations of dynamics:

$$\rho u_i u_j=2\mu_T\left[\frac{1}{2}\left(\frac{\partial \overline{u_i}}{\partial x_j}+\frac{\partial \overline{u_j}}{\partial x_i}\right)-\frac{1}{3}\frac{\partial \overline{u_k}}{\partial x_k}\delta_{ij}\right]-\frac{2}{3}\rho k\delta_{ij},$$

Where δ_{ij} —Kronecker symbol.

Using empirical closure coefficients of these equations allows a numerical solution of the turbulent fluid flow in the computational domain.

The following equation is required to calculate the pump head:

$$H = \frac{p_2}{\rho g} + \frac{V_2^2}{2g} - \frac{p_1}{\rho g} - \frac{V_1^2}{2\rho},$$

Where p_2 — pressure at the outlet of the first stage guide vane;

p_1 — pump inlet pressure;

V_2 — Average speed at the exit of the first stage guide vane;

V_1 — Average speed at the pump inlet.

In the numerical model, the rotor speed and pump feed are set.

Turbulent fluid flow prevails in the flow part of the pump.

For the region of fluid flow that rotates with the rotor, the equation of change in momentum is written as follows:

$$\rho\left[\frac{\partial \overline{w_i}}{\partial t} + \overline{u_j}\frac{\partial \overline{w_i}}{\partial x_j}\right] = -\frac{\partial \overline{p}}{\partial x_i} + \frac{\partial}{\partial x_i}\left[T_{ij}^{(v)} - \rho w_i w_j\right] + F_u + F_\kappa,$$

Where $F_u = \rho\omega^2 r$ —the tension forces of inertia;

$F_\kappa = 2\omega w_{xy}$ —Coriolis force tension.

The calculation of the pump parameters was carried out in the following sequence: first, the calculation was carried out in a stationary setting, and after the relative convergence of the parameters — non-stationary. This approach can significantly reduce the time of hydrodynamic calculation.

To compare the cavitation characteristics of the pump in different operating modes, the cavitation speed coefficient given by S.S. Rudnev, is calculated by the formula:

$$C_k = \frac{5,62n\sqrt{Q}}{\Delta h^{\frac{3}{4}}}$$

Practical part.

The 3D model of the calculated area is imported in the Parasolid (*) format.x_b). The first (most cavitation-prone) stage of a multistage centrifugal pump, which includes three subregions (regions): inlet, impeller, and guide vane, is taken as the calculation area. In this case, the pump inlet was applied in a special form, previously optimized for such multistage pumps [10].

This simulation does not take into account fluid flows between regions and flows in the space between the casing and the impeller disks. Such assumptions greatly simplify the calculation, but slightly reduce the accuracy of the calculation.

Figure 1 shows the imported model of the computational domain.

All boundaries are walls, except for the entrance to the pump (Inlet) and exit from the stage (Outlet). The types of boundaries for them are presented in table 1.

For the calculation, the following grid construction parameters are used (Table 2).

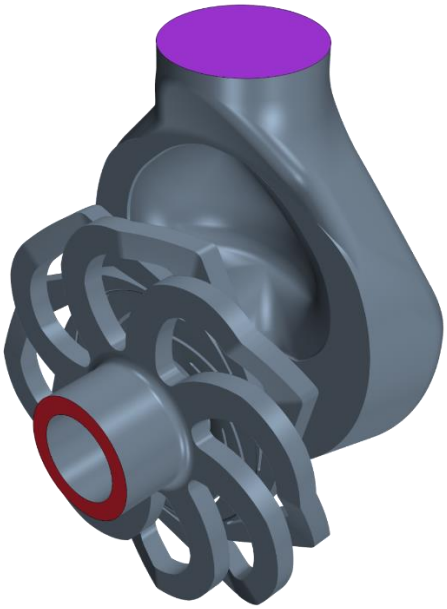

Figure 1. Imported three-dimensional model of the calculated area of the flow part of the first stage of the pump.

Table 1. Correspondence of borders with their types.

Border name	New type
Outlet	Input speed
Inlet	Input stagnation

Table 2. The main parameters of grid construction.

Parameter	Property	Value
Base	Value	3,5 мм
Prismatic layer thickness> Relative size	Absolute	1,5 мм
Surface Size> Relative minimum size	Percentage of base	25
Surface Size> Relative Desired Value	Percentage of base	100
Prismatic Stretching	Value	1.3
The number of prismatic layers	Value	5

In the region of the impeller, the values of the fluid flow rates reach their maximum mark, which causes the largest velocity gradients in this region. This circumstance significantly affects the calculation, therefore, the grid of this area needs to be crushed for a more accurate calculation.

The mesh parameters of the impeller region are presented in table 3.

In total, the regions were divided into 546083 cells, of which 231494 cells in the region of the impeller, 246832 cells in the guide vane and 67757 cells in the inlet.

Figure 2 shows the cross section of the areas of the impeller and the guide apparatus.

Table 3. Parameters of the impeller construction grid

Parameter	Property	Value
Surface Size> Relative minimum size	Percentage of base	20
Surface Size> Relative Desired Value	Percentageofbase	50

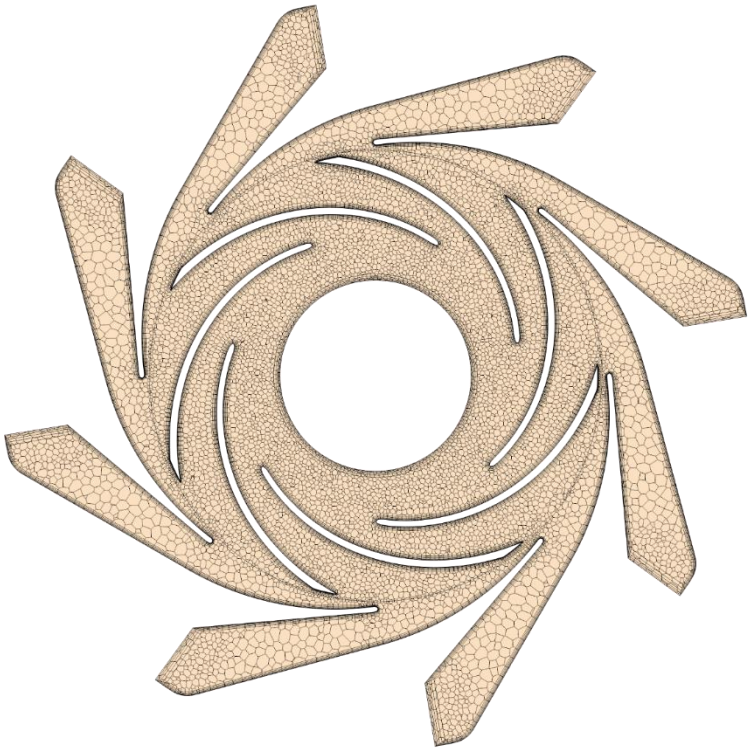

Figure 2. The cross section of the impeller with the guide apparatus of the grid model of the calculation area.

The following models were used in the calculation:
• Time-non-stationary task;
• working environment — Euler multiphase;
• Euler multiphase model — volume of fluid (VOF);
• Solver — divided;
• Flow regime — turbulent;
• k-epsilon turbulence model. The phases selected are water and steam. The value of the saturation pressure of the water selected value p = 2338 Pa, corresponding to 20 ° C.

Results

In the process of hydrodynamic modeling, scenes of the distribution of the vapor phase in the computational domain are created for clarity. Figure 3 shows the distribution of the vapor phase during non-cavitation operation of the pump, and Figure 4 — in the cavitation mode.

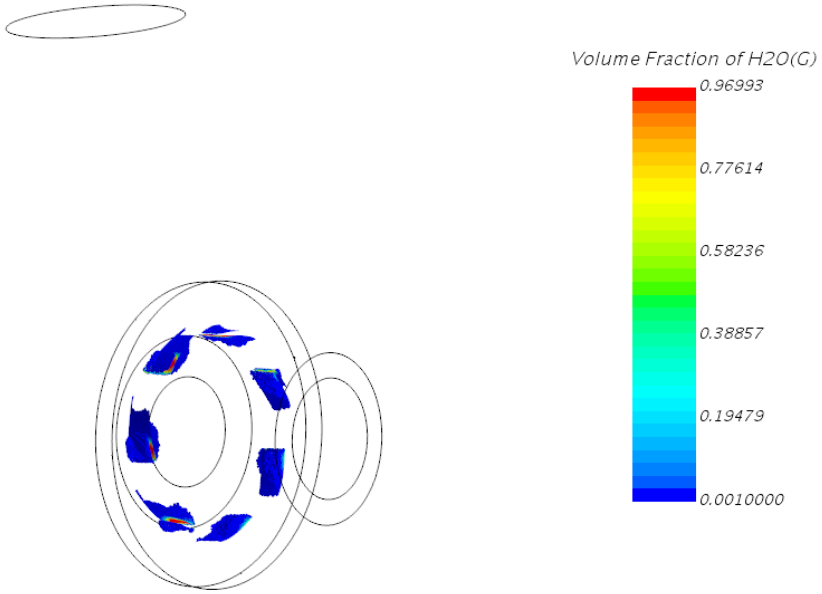

Figure 3. Distribution of the vapor phase in the non-cavitation operation of the pump.

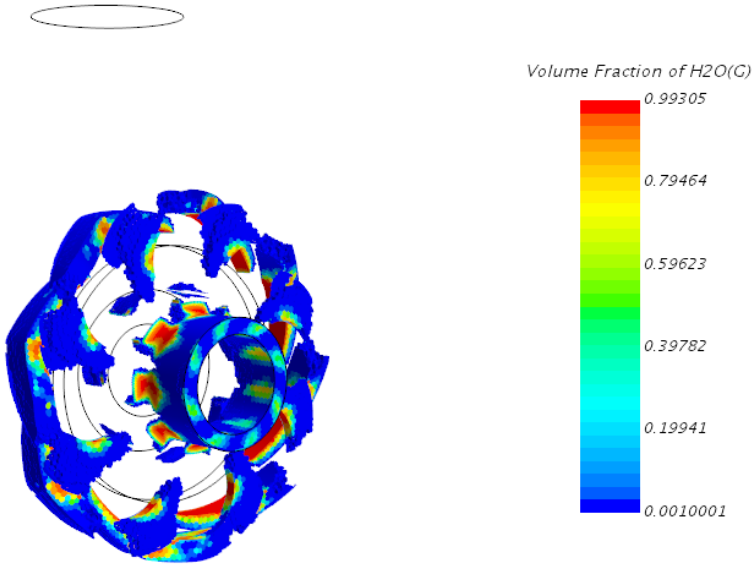

Figure 4. Distribution of the vapor phase in the cavitation mode.

The first basic operating mode of the pump of this hydrodynamic simulation is the point in the optimal operating mode of the pump: the pump rotor speed n = 7000 rpm at a flow rate in the system is $Q = 100\frac{м^3}{h}$. As a result, it is obtained a graph of the partial cavitation characteristics of the pump with these parameters (Fig. 5). Cavitation margin value for the second critical pump mode is $\Delta h = 13,3 м.$

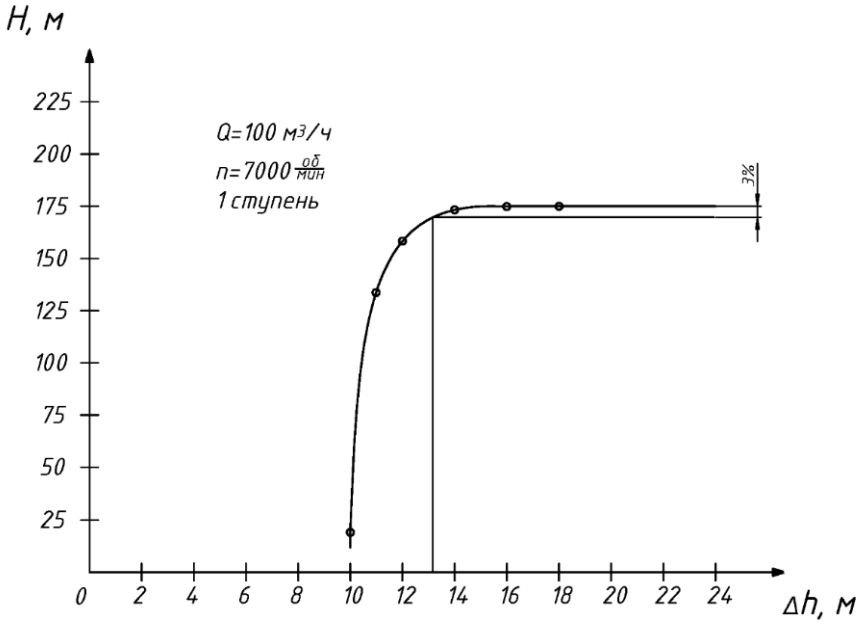

Figure 5. Cavitation characteristic of the pump at $n = 7000\frac{об}{мин}$

The second operating point has the following parameters: pump rotor speed is $n = 5500\,rpm$ at a flow rate of $Q = 100\frac{м^3}{h}$. The graph of the particular cavitation characteristic is shown in Figure 6. The value of the cavitation reserve is $\Delta h = 8,2\,м.$

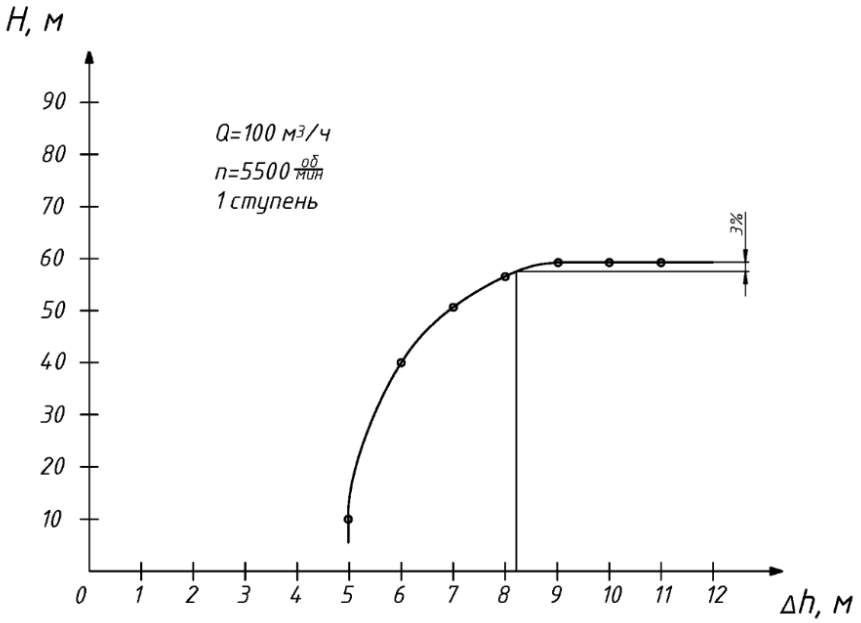

Figure 6. Cavitation characteristic of the pump at $n = 5500\frac{об}{мин}$

The third working point with the minimum engine rotor speed after the gear ratio of the multiplier has the following parameters: pump rotor speed is $n = 4000\,rpm$ at a flow rate of $Q = 100\frac{м^3}{h}$. The graph of the particular cavitation characteristic is shown in Figure 7. The value of the cavitation reserve is $\Delta h = 8,7\,м$.

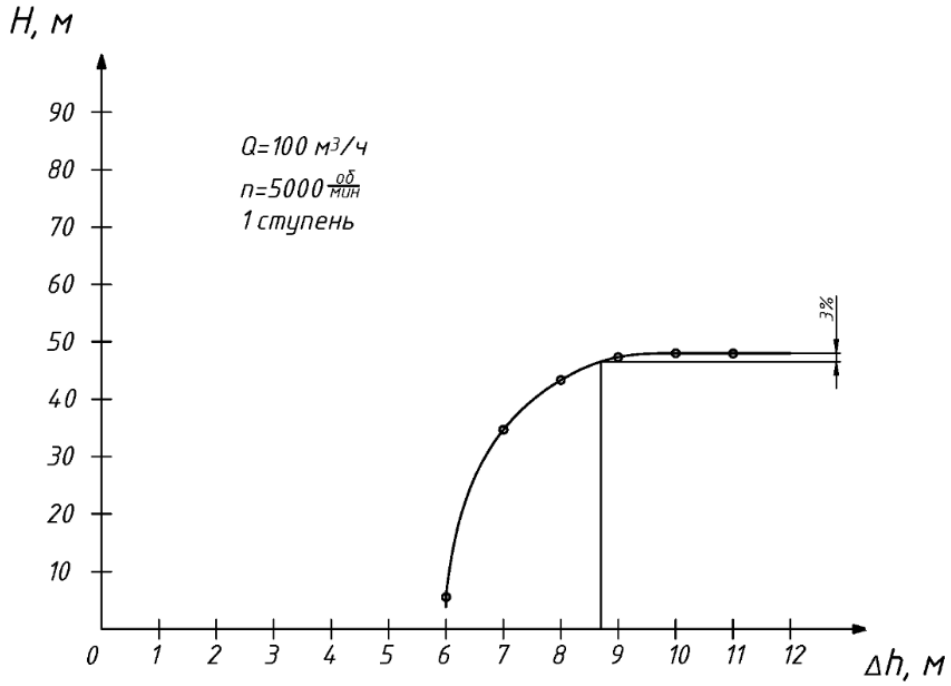

Figure 7. Cavitation characteristic of the pump at $n = 4000\,rpm$

The results of calculating the cavitation characteristics of the pump, as well as the calculated cavitation coefficient of speed are presented in table 4.

Table 4. Cavitation characteristics of the pump in different operating modes.

Name	Flow rate, cubic m / h	Head, m	Cavitation reserve, m	Cavitational speed coefficient
At $n = 5000\,rpm$	100	48	8,7	928
At $n = 5500\,rpm$		60	8,2	1067
At $n = 7000\,rpm$		175	13,3	945

Figure 8 shows a graphical display of the tabular data.

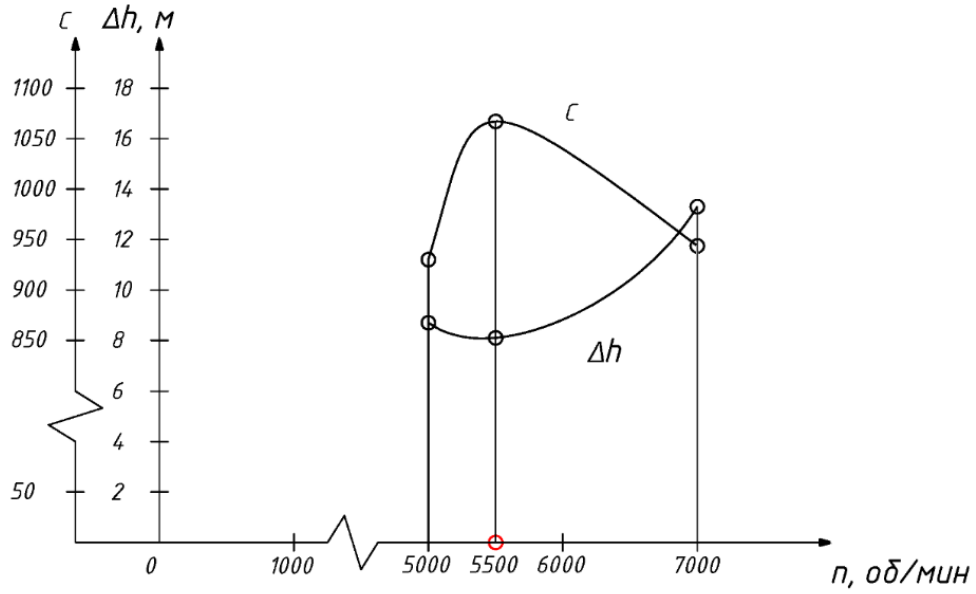

Figure 8. Graphs of the dependences of the cavitation stock and cavitation coefficient of speed on the rotational speed of the pump rotor.

Conclusion

The results obtained show that a decrease in the rotor speed of the pump rotor with a constant feed value can somewhat reduce the allowable cavitation reserve of the pump. But at the same time, the pressure value of the pump drops sharply, since the pump is operating in a non-optimal mode.

Also, on the graph, it can be noticed an inverse relationship: when a certain value of the rotor speed of the pump is reached, the cavitation characteristics begin to deteriorate. This phenomenon is due to the fact that the fluid flow rate to a large extent begins to differ from the rotational speed of the impeller, thereby the impeller no longer transfers energy to the flow, but instead takes it. A flow throttling phenomenon occurs in the flow part, in which cavitation is actively developing, which is the reason for the deterioration of cavitation characteristics.

Therefore, for a pump of this type, the proposed method for increasing cavitation characteristics is in principle permissible, but only with a slight, no more than 20%, decrease in the rotor speed of the pump. With a further decrease in cavitation characteristics again begin to deteriorate.

List of references

[1] A Protopopov and D Bondareva 2019 *IOP Conf. Ser.: Mater. Sci. Eng*. 492 012002
[2] A Protopopov and V Vigovskij 2019 *IOP Conf. Ser.: Mater. Sci. Eng*. 492 012003
[3] V Lomakin et al 2019 *IOP Conf. Ser.: Mater. Sci. Eng.* 492 012012
[4] N Egorkina and APetrov 2019 *IOP Conf. Ser.: Mater. Sci. Eng.* 492 012015
[5] N Isaev 2019 IOP *Conf. Ser.: Mater. Sci. Eng.* 492 012026
[6] A Protopopov and C Jakovich 2019 *IOP Conf. Ser.: Mater. Sci. Eng.* 492 012034
[7] A Petrov et al 2019 *IOP Conf. Ser.: Mater. Sci. Eng.* 492 01203
[8] T Valiev and APetrov 2019 *IOP Conf. Ser.: Mater. Sci. Eng.* 492 012038
[9] V Cheremushkin and V Lomakin 2019 *IOP Conf. Ser.: Mater. Sci. Eng.* 492 012039
[10] *Petrov A., Lysenko A., Valiev T., Isaev N.* Optimal design of inlet device of multistage centrifugal pump. IOP Conference Series: Materials Science and Engineering 2019. — Vol. 492, Issue 1. — Art. no 012040; DOI: 10.1088/1757-899X/492/1/012040.